SUMMARY OF APATITE FISSION-TRACK ANALYSES AND RADIOMETRIC DATES FROM THE NECHAKO REGION, BRITISH COLUMBIA (NTS 92O, N; 93B, C, E, F, G, L) AND IMPLICATIONS FOR OIL AND GAS PROSPECTIVITY

J.M. Riddell[1]

ABSTRACT

The Nechako Geoscience Project of the BC Ministry of Energy, Mines and Petroleum Resources' Oil and Gas Division began in 2004. Fieldwork and sample gathering ended in 2007, and sample analyses are largely complete. Interpretation and publication of data continues. This paper presents a summary of 17 radiometric dates and 69 apatite fission-track analyses completed during the life of the project. New radiometric ages from surface outcrops and wells provide constraints on the distribution of prospective rocks and the locations of important structures. Apatite fission-track (AFT) ages constrain the time limits of a rock's most recent passage through the oil and gas windows. The AFT data for each sample indicate whether it has been heated enough for hydrocarbon generation since trap-forming compressional tectonic events occurred in the central Cordillera.

Riddell, J.M. (2010): Summary of apatite fission-track analyses and radiometric dates from the Nechako region, British Columbia, and implications for oil and gas prospectivity; *in* Geoscience Reports 2010, *BC Ministry of Energy, Mines and Petroleum Resources*, pages 123–131.

[1]Resource Development and Geoscience Branch, BC Ministry of Energy, Mines and Petroleum Resources, Victoria, BC

Key Words: Nechako Basin, apatite fission-track analyses, thermochronology, U-Pb radiometric dates, hydrocarbon generation, oil and gas window

INTRODUCTION

The Nechako Geoscience Project began in 2004 with the goal of assessing the oil and gas potential of the Nechako region, specifically by evaluating critical factors of a petroleum system: the quality of petroleum source and reservoir rocks, an appropriate thermal history, and timing of potential trap formation and petroleum migration. The project involved fieldwork and sampling, regional stratigraphic correlations, thermal history studies and radiometric and fossil dating. The integration of these results with those of concurrent Nechako geoscience projects led by the Geological Survey of Canada, Geoscience BC and other partners, is ongoing.

Previous publications generated by the project have reported on fieldwork, surface geology, vitrinite reflectance and palynology (Ferri and Riddell, 2006; Riddell et al., 2007; Riddell and Ferri, 2008) and reservoir quality (Brown et al., 2008).

This paper presents a summary of radiometric dates and apatite fission-track analyses completed during the life of the project. Comprehensive analytical datasets from these studies will be released this year as open file publications.

Early Jurassic to Early Eocene formations host potential source and reservoir units in the region, so an understanding of their distribution and structure is important to the assessment of their oil and gas potential. However, in the Nechako region, rocks older than the volcanic and sedimentary rocks of the Early Eocene Ootsa Lake Group are poorly exposed and structures cannot be mapped directly. The radiometric dates and apatite fission-track analyses summarized here provide constraints on the distribution of prospective rocks and the locations of important structures.

We can infer the regional tectonic history of the covered area by assuming continuity with the areas along the strike of the Cordillera to the northwest and southeast. A large-scale compressional-transpressional regime was active from the mid-Cretaceous to the earliest Tertiary during the accretion of outboard terranes to North America. Events associated with this regime are expressed along the Intermontane Belt (in the Bowser Basin to the northwest of Nechako and in the Chilcotin Mountains to the southeast) as thrust faults and folds and by accumulations of synorogenic clastic deposits of locally derived detritus on angular unconformities (Schiarizza et al., 1997; Evenchick et al., 2007). In the Chilcotin Mountains, the main contractional structures predate the Cenomanian and younger Powell Creek formation (Schiarizza et al., 1997, 2003). In

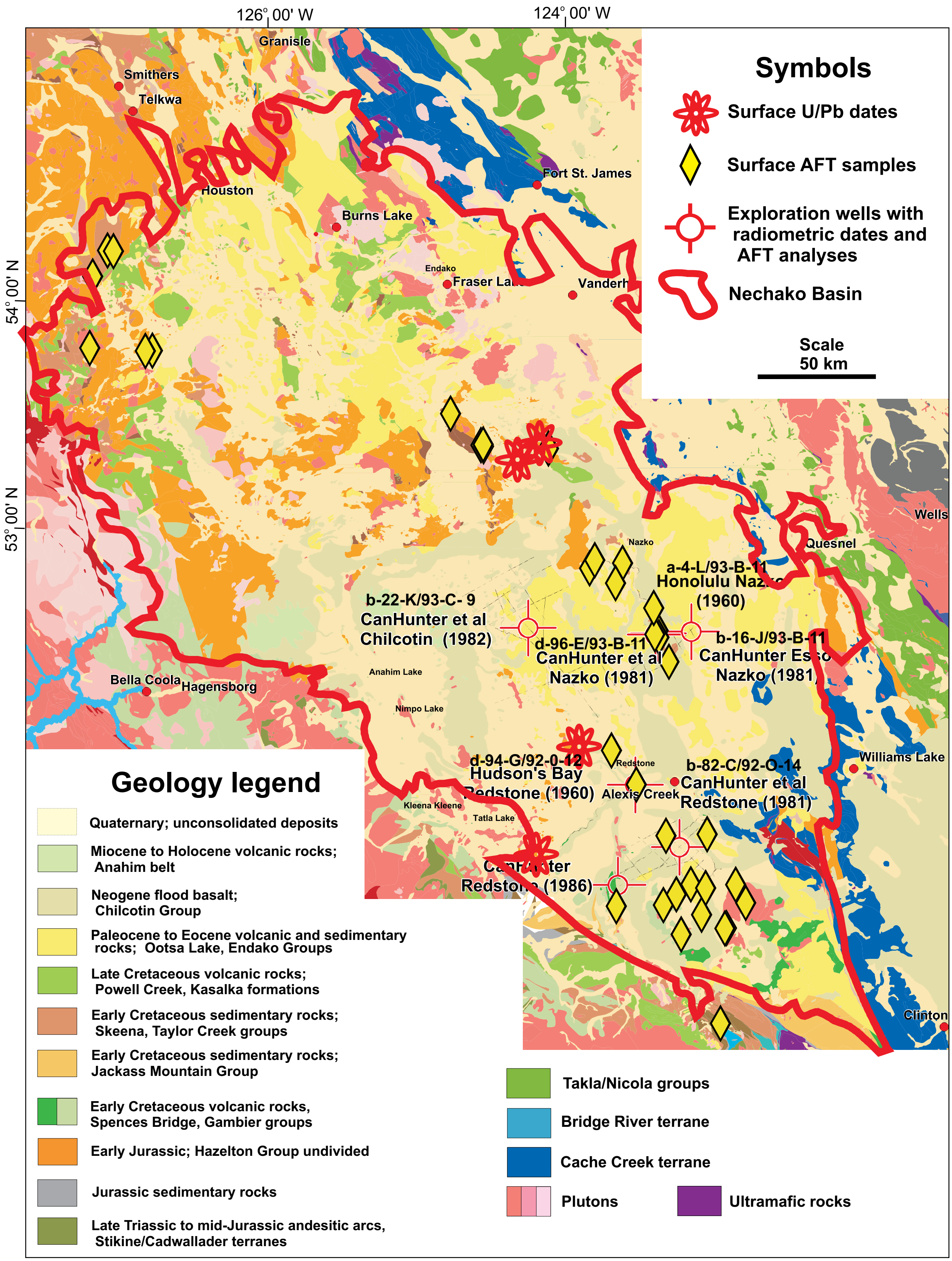

Figure 1. Nechako Basin map with radiometric and AFT sample locations.

the Bowser Basin, evidence of thrust faulting and clastic deposition continued until the Maastrichtian (Evenchick et al., 2007). The shift to Eocene transtensional tectonics is marked along the Intermontane Belt by continued and significant dextral movement along steeply dipping strike-slip structures such as the Pinchi, Fraser–Straight Creek, Yalakom and associated faults, and unroofing of metamorphic core complexes such as the Wolverine (Struik, 1993), Tatla Lake (Friedman and Armstrong, 1988) and Vanderhoof (Grainger et al., 2001) complexes. The initiation of strike-slip movement is documented in the Chilcotin Mountains beginning sometime between 70 and 65 Ma, and continuing until about 35 Ma (Umhoefer and Schiarizza, 1996). Eocene normal faulting is mapped in the south part of the Bowser Basin (O'Sullivan et al., 2009) and is inferred from interpretations of magnetic and paleomagnetic data (Lowe et al., 2001) in the Endako region.

Similar structural patterns are assumed to underlie the covered areas of the Nechako. The loci and timing of these inferred structures have direct implications for oil and gas prospectivity. Favourable conditions for the construction of important components of functioning petroleum systems would have occurred during the compressional regime; deposition of coarse clastic reservoir units, the formation of fold and thrust-fault traps, and the burial/heating of potential source-rock units. During the Eocene transtensional regime, the deposition of volcanic, volcaniclastic and clastic sedimentary rocks of the Ootsa Lake Group may have buried and heated prospective Mesozoic source-rock units. Clastic rocks in these Eocene sequences represent additional potential reservoir units. However, Eocene movement along steeply dipping strike-slip faults would have a detrimental effect on oil and gas prospectivity by introducing vertical conduits from hydrocarbon traps to the surface, and by fragmenting plays.

RADIOMETRIC DATES

Table 1 summarizes data from 17 U-Pb radiometric zircon dates from plutonic and volcanic rocks from the Interior Plateau of south-central British Columbia. Four samples are from surface outcrops and 13 are from archived oil and gas exploration well cuttings and core. The samples were analyzed to address stratigraphic questions about the underlying, poorly exposed Mesozoic and early Cenozoic

TABLE 1. SUMMARY OF 17 RADIOMETRIC DATES*

Field label	Report # (A to Z lab #)	Location	Easting UTM NAD 83 Zone 10	Northing UTM NAD 83 Zone 10	Rock type	Sample type	U/Pb age (or youngest population)	Geological implications
Sub-surface samples								
a-4-L 10625-10864 ft	965-03	Honolulu Nazko well (a-4-L/93-B-11)	471599	5835406	Diorite	igneous	170.8 ± 0.8	mid-Jurassic pluton, co-eval with Stag Lake Stock and Spike Peak Stock
b-16-J 1060-1120m	738-27 (2-2)	CanHunter Esso Nazko well (b-16-J/93-B-11)	486398	5836290	Clastic rocks with tuff and ash	detrital	57.0 ± 2.5	Paleocene or younger deposition above 1720 m
b-16-J 1640-1720m	738-28 (2-3)				Clastic rocks with tuff and ash	detrital	57.5 ±1.4	Volcanics at well-base are early Cretaceous, correlation unknown
b-16-J 2300-2385m	738-30 (2-5)				Volcaniclastic tuffs and ash	igneous	140.6 ± 1.6	
b-22-K 2020-2095m	738-45 (5-3)	Canhunter et al. .Chilcotin (b-22-K/93-C-14)	413936	5837969	Ash tuff	igneous	52.4 ± 1.6	Early Tertiary from 2020 to 3745 m Mainly Early Eocene Ootsa Lake volcanics
b-22-K 2570-2670m	738-44 (5-2)				Andesite flow	igneous	54.0 ± 2.1	
b-22-K 3119-3124.5m	824				Flow or tuff	igneous	60.3 ± 2.2	
b-22-K 3625-3745m	738-43 (5-1)				Fragmental volcanic	igneous	50.6 ±1.6	
b-82-C 635-730m	738-49 (6-3)	CanHunter et al Redstone (b-82-C/92-O-14)	480980	5740701	Siltstone	detrital	101.7 ± 2.2	Deposition is Albian or later, dominant source terrane is Albian Granite at well-base is Albian-aged
b-82-C 1100-1200m	805-01				Siltstone, claystone, sst	detrital	107.3 ± 0.9	
b-82-C 1640-1700m	738-47 (6-1)				Granite	igneous	101.4 ± 1.9	
d-94-G 2050-2160m	738-36 (3-6)	CanHunter Redstone (d-94-G/92-O12)	453711	5723900	Andesite	igneous	93.7 ± 3.2	Andesite at well-base could be Powell Creek Volcanics, OR Spences Bridge Group
d-96-E 3180-3320m	805-02	CanHunter et al. Nazko (d-96-E/93-B-11)	470283	5834950	Volcaniclastic lithic tuffs	igneous	150.2 ± 3.1	Volcanics are Late Jurassic. A possible correlation is Nechako volcanics
Surface samples								
FF05-85	857-05	Puntzi Lake	434471	5785920	andesite	igneous	101.1 ± 2.2	Probably Spences Bridge Group volcanics
FF06-66	857-04	Batnuni Lake	413345	5917087	tuff	igneous	161.6 ± 2.4	Probably Bowser Lake Gp, possibly Hazelton
JR06-28	857-09	Batnuni Cone	422969	5917545	rhyolite	igneous	48.51 ± 0.99	Ootsa Lake Group
JR06-112	857-12	Choelquoit Lake	422274	5731989	andesite	igneous	101.1 ± 2.8	Probably Spences Bridge Group volcanics

*Surface samples were collected in 2005 and 2006; locations on Figure 1. Archived well cuttings were sampled in 2006. Analyses were performed by Apatite to Zircon, Inc. of Viola, Idaho.

stratigraphy, and to constrain timing and location of important structures. In some locations, apatite fission-track samples were collected concurrently. The specific implications of the results of U-Pb zircon dates for individual samples will be discussed in detail in a forthcoming open file publication. Some general implications about regional scale structures can be made:

- Four Paleocene to Early Eocene dates were returned from cuttings from the CanHunter et al. Chilcotin well (b-22-K/93-C-14) at depths between 2020 and 3745 m. This represents an anomalously thick section of early Paleogene and younger deposits, and may represent the location of an Eocene pull-apart basin between two en-echelon strike-slip faults. The same interpretation is made by Hayward and Calvert (in prep) based on observations of Canadian Hunter seismic and gravity surveys of the early 1980s. Bouguer low-gravity anomalies and magnetic lineations show that the well is within a rhomboidal basin.
- Two detrital and one igneous sample from the well cuttings of the CanHunter et al. Redstone well (b-82-C/92-O-14) produced ages between 101 and 108 Ma, putting them in Albian time. Granite at the base of the well is about the same age as the detrital zircons in overlying coarse clastic sediment. This is similar to what is observed during Albian time in the Bowser Basin to the north (Evenchick et al., 2007) and in the Chilcotin Mountains to the south; the peak of compressional tectonics along the Cordillera was accompanied by magmatism, concurrent rapid uplift and shedding of local detritus into adjacent basins. This is an important time in the region for the deposition of Cretaceous reservoir beds, formation of structural traps and maturation of potential source rocks by burial.
- Two surface samples from Puntzi Lake and Choelquoit Lake produced very similar ages of around 101 Ma. Both samples came from outcrops of purple and green andesitic flows and breccia that were originally mapped by Tipper (1959, 1968) as the Jurassic Hazelton Group. The new dates indicate that they are actually part of a broad but poorly exposed belt of mid-Cretaceous volcanic rocks that also crops out in the Taseko Lake map area (92O) to the east-southeast (Hickson and Higman, 1993; Riesterer et al., 2001; Schiarizza et al., 2002), where they have been correlated with the Spences Bridge Group.

APATITE FISSION-TRACK ANALYSES

Results of 69 surface and subsurface apatite fission-track analyses are summarized in Table 2. Apatite fission-track data are used for oil and gas studies because the temperature range over which track annealing occurs, 60° to 160°C (Ketcham et al., 1999), is about the same as temperatures required for oil and gas generation. Apatite fission-track ages can thereby be used to constrain the time limits of a rock's most recent cooling through the oil and gas windows. Samples with more than one species of apatite, such as detrital samples with mixed source terrains, can contain multiple apatite geothermometers in a single sample, and can provide improved detail of the sample's cooling history.

The implications of AFT analyses for individual samples or sample sets will be discussed in detail in a forthcoming open file publication. Some general implications about regional scale structures can be made:

Figure 2 is a histogram of the oldest apatite dates from samples from the Nechako region. The oldest apatite age of a given sample indicates the earliest period of cooling through the annealing temperature of apatite. The smaller, flatter peak between 75 and 125 Ma shows samples that cooled following compressional events of the mid-Mesozoic and were not reheated again before the present. The larger histogram peak at about 50 Ma represents rocks that either formed or were reheated enough to anneal older apatite fission tracks during magmatic and volcanic events associated with the transtensional regime of the Paleocene and Eocene.

TABLE 2. SUMMARY OF 69 APATITE FISSION-TRACK SAMPLES*

Field label	A2Z Sample Number	Easting	Northing	Apatite grains observed	Data Quality 1=poor 10=excellent	Age of Oldest Apatite Fission Track (Ma)	Timing of Initiation of Uplift/Cooling (Ma)	Pooled Fission-Track Age (Ma) (Zircon U/Pb Age)	Sample type
FF05-17	738-01	499257	5662348	1000s	7	Dpar (μm)=1.68: 106 ± 11.4	Dpar (μm)=1.68: ≥106 ± 11.4	82.5 ± 8.9	detrital
FF05-32	738-02	453115	5714378	1000s	8	Dpar (μm)=1.68: 79.5 ± 3.5	Dpar (μm)=1.68: ≥79.5 ± 3.5	64.2 ± 2.8	detrital
FF05-38	738-03	475060	5745563	1000s	7	Dpar (μm)=1.60: 51.1 ± 3.5 Dpar (μm)=2.53: 52.6 ± 8.6	Dpar (μm)=1.60: ≥51.1 ± 3.5 Dpar (μm)=2.53: ≥52.6 ± 8.6	52.3 ± 3.3	detrital
FF05-39	738-04	491015	5710508	10s	4	Dpar (μm)=1.40: 42.1 ± 5.4	Dpar (μm)=1.40: ≥42.1 ± 5.4	42.7 ± 5.5	igneous
FF05-40	738-05	481831	5701760	1000s	7	Dpar (μm)=1.67: 100.0 ± 12.6	Dpar (μm)=1.67: ≥100.0 ± 12.6	88.0 ± 10.8	igneous
FF05-44	738-06	473928	5714838	1000s	3	Dpar (μm)=1.52: 81.5 ± 4.1	Dpar (μm)=1.52: ≥81.5 ± 4.1	77.0 ± 3.9	igneous
FF05-48	738-07	486174	5724102	10s	2	Dpar (μm)=1.48: 53.8 ± 4.7	Dpar (μm)=1.48: ≥53.8 ± 4.7	55.6 ± 4.9	igneous
FF05-49	738-08	479689	5719593	1000s	9	Dpar (μm)=1.33: 68.8 ± 4.7	Dpar (μm)=1.33: ≥68.8 ± 4.7	70.4 ± 4.8	igneous
FF05-51	738-09	492762	5722331	<20	2	Dpar (μm)=1.46: 53.8 ± 9.0	Dpar (μm)=1.46: ≥53.8 ± 9.0	58.1 ± 9.7	igneous
FF05-52	738-10	506063	5723902	1000s	8	Dpar (μm)=1.38: 53.9 ± 5.1	Dpar (μm)=1.38: ≥53.9 ± 5.1	53.9 ± 5.1	igneous
FF05-54	738-11	510496	5715757	1000s	1	Dpar (μm)=1.72: 31.3 ± 1.4	Dpar (μm)=1.72: ≥31.3 ± 1.4	32.4 ± 1.4	igneous
FF05-55	738-12	501888	5704608	1000s	4	Dpar (μm)=1.40: 39.5 ± 1.8	Dpar (μm)=1.40: ≥39.5 ± 1.8	38.2 ± 1.7	igneous
FF05-56	738-13	501319	5704419	100s	2	Dpar (μm)=1.38: 28.6 ± 1.7	Dpar (μm)=1.38: ≥28.6 ± 1.7	28.1 ± 1.7	igneous
FF05-57	738-14	493405	5746187	<10	1	Dpar (μm)=1.44: 31.0 ± 4.7	Dpar (μm)=1.44: ≥31.0 ± 4.7	29.5 ± 4.5	igneous
FF05-60	738-15	437930	5869933	100s	1	Dpar (μm)=1.56: 41.0 ± 6.5 Dpar (μm)=2.24: 55.0 ± 12.1	Dpar (μm)=1.56: ≥41.0 ± 6.5 Dpar (μm)=2.24: ≥55.0 ± 12.1	37.7 ± 4.8	detrital
FF05-66	738-16	441154	5864344	100s	5	Dpar (μm)=1.51: 30.7 ± 3.5	Dpar (μm)=1.51: ≥30.7 ± 3.5	31.6 ± 3.6	igneous
FF05-70	738-17	472028	5833656	100s	6	Dpar (μm)=1.42: 105.0 ± 4.2 Dpar (μm)=2.17: 106.0 ± 5.3	Dpar (μm)=1.42: ≥105.0 ± 4.2 Dpar (μm)=2.17: ≥106.0 ± 5.3	97.4 ± 3.5	detrital
FF05-71	738-18	470252	5835011	<10	3	Dpar (μm)=1.64: 119.0 ± 11.8	Dpar (μm)=1.64: ≥119.0 ± 11.8	83.9 ± 8.2	detrital
FF05-76	738-19	469775	5846631	100s	5	Dpar (μm)=1.48: 120.0 ± 10.2 Dpar (μm)=2.38: 121.0 ± 9.8	Dpar (μm)=1.48: ≥120.0 ±10.2 Dpar (μm)=2.38: ≥121.0 ± 9.8	91.8 ± 3.5	detrital
FF05-78	738-20	455908	5866539	<5	3	Dpar (μm)=1.72: 147 ± 38	Dpar (μm)=1.72: ≥147 ± 38	190.9 ± 58.0	detrital
FF05-81	738-21	451001	5783484	1000s	5	Dpar (μm)=1.35: 38.9 ± 2.0 Dpar (μm)=2.00: 39.3 ± 2.7	Dpar (μm)=1.35: ≥38.9 ± 2.0 Dpar (μm)=2.00: ≥39.3 ± 2.7	40.4 ± 1.8	detrital
FF05-82	738-22	461976	5768349	1000s	4	Dpar (μm)=1.56: 50.1 ± 3.2 Dpar (μm)=2.21: 52.3 ± 5.7	Dpar (μm)=1.56: ≥50.1 ± 3.2 Dpar (μm)=2.21: ≥52.3 ± 5.7	49.8 ± 2.8	detrital
1-1 (c-75-A 3820–3850')	738-23	461398	5768336	<20	3	Dpar (μm)=1.38: 32.5± 4.9 Dpar (μm)=2.30: 33.4 ± 5.1	Dpar (μm)=1.38: ≥32.5 ± 4.9 Dpar (μm)=2.30: ≥33.4 ± 5.1	31.0 ± 3.3	detrital
1-2 (c-75-A 2610–2900')	738-24	461398	5768336	100s	5	Dpar (μm)=1.73: 40.5 ± 3.1 Dpar (μm)=2.81: 52.5 ± 5.0	Dpar (μm)=1.73: ≥40.5 ± 3.1 Dpar (μm)=2.81: ≥52.5 ± 5.0	40.8 ± 2.5	detrital
1-3 (c-75-A 1050 –1300')	738-25	461398	5768336	100s	5	Dpar (μm)=1.31: 45.7 ± 4.4 Dpar (μm)=2.04: 49.5 ± 5.1	Dpar (μm)=1.31: ≥45.7 ± 4.4 Dpar (μm)=2.04: ≥49.5 ± 5.1	42.5 ± 2.9	detrital
2-1 (b-16-J 520 – 580 m)	738-26	480980	5740701	1000s	8	Dpar (μm)=2.00: 54.4 ± 4.2 Dpar (μm)=2.75: 55.8 ± 4.9	Dpar (μm)=2.00: ≥54.4 ± 4.2 Dpar (μm)=2.75: ≥55.8 ± 4.9	53.6 ± 3.2	mixed igneous and detrital
2-2 (b-16-J_1060 – 1120 m)	738-27	480980	5740701	100s	6	Dpar (μm)=1.57: 64.0 ± 8.3 Dpar (μm)=2.30: 64.9 ± 4.8	Dpar (μm)=1.57: ≥64.0 ± 8.3 Dpar (μm)=2.30: ≥64.9 ± 4.8	58.5 ± 3.8	detrital
2-3 (b-16-J 1640 – 1720 m)	738-28	486398	5836290	100s	7	Dpar (μm)=1.88: 52.5 ± 3.3	Dpar (μm)=1.88: ≥52.5 ± 3.3	50.1 ± 3.1	detrital
2-4 (b-16-J 2020 – 2090 m)	738-29	486398	5836290	100s	5	Dpar (μm)=1.88: 56.5 ± 6.8 Dpar (μm)=2.53: 59.2 ± 7.7	Dpar (μm)=1.88: ≥56.5 ± 6.8 Dpar (μm)=2.53: ≥59.2 ± 7.7	62.0 ± 5.6	igneous
2-5 (b-16-J 2300 – 2385 m)	738-30	486398	5836290	100s	4	Dpar (μm)=1.64: 44.0 ± 3.2 Dpar (μm)=2.59: 57.4 ± 17.4	Dpar (μm)=1.64: ≥44.0 ± 3.2 Dpar (μm)=2.59: ≥57.4 ± 17.4	31.6 ± 2.2	mixed

**Surface samples were collected 2005 - 2007; locations on Figure 1. Archived well cuttings were sampled in 2006. Analyses were performed by Apatite to Zircon, Inc. of Viola, Idaho. Data with A2Z sample numbers with 738 and 867 prefixes were modeled using AFTSolve v1.4.1. software. Data with A2Z sample numbers with 910 and 965 prefixes were modeled using HeFTY v1.6.7. software.*

TABLE 2 CONTINUED

Field label	A2Z Sample Number	Easting	Northing	Apatite grains observed	Data Quality 1=poor 10=excellent	Age of Oldest Apatite Fission Track (Ma)	Timing of Initiation of Uplift/Cooling (Ma)	Pooled Fission-Track Age (Ma) (Zircon U/Pb age)	Sample type
3-1 (d-94-G 30 – 100 m)	738-31	453711	5723900	100s	3	Dpar (μm)=1.23: 44.0 ± 5.4 Dpar (μm)=2.18: 45.8 ± 4.2	Dpar (μm)=1.23: ≥44.0 ± 5.4 Dpar (μm)=2.18: ≥45.8 ± 4.2	44.2 ± 3.4	detrital
3-2 (d-94-G 635 – 725 m)	738-32	453711	5723900	100s	5	Dpar (μm)=1.44: 59.5 ± 2.9 Dpar (μm)=2.12: 104 ± 22	Dpar (μm)=1.44: ≥59.5 ± 2.9 Dpar (μm)=2.12: ≥104 ± 22	51.4 ± 2.5	detrital
3-3 (d-94-G 1080 –1180 m)	738-33	453711	5723900	100s	5	Dpar (μm)=1.48: 52.5 ± 2.7	Dpar (μm)=1.48: ≥52.5 ± 2.7	46.8 ± 2.4	detrital
3-4 (d-94-G 1470 –1600 m)	738-34	453711	5723900	10s	5	Dpar (μm)=1.40: 33.8 ± 3.2 Dpar (μm)=1.94: 35.5 ± 6.7	Dpar (μm)=1.40: ≥33.8 ± 3.2 Dpar (μm)=1.94: ≥35.5 ± 6.7	31.4 ± 2.6	detrital
3-5 (d-94-G 1800 –1880 m)	738-35	453711	5723900	100s	5	Dpar (μm)=1.47: 42.0 ± 2.6 Dpar (μm)=2.30: 121 ±1 9.4	Dpar (μm)=1.47: ≥42.0 ± 2.6 Dpar (μm)=2.30: ≥121 ± 19.4	39.1 ± 2.4	detrital
3-6 (d-94-G 2050 –2160 m)	738-36	453711	5723900	<20	3	Dpar (μm)=1.52: 47.2 ± 15.1 Dpar (μm)=2.07: 58.5 ± 17.8	Dpar (μm)=1.52: ≥47.2 ± 15.1 Dpar (μm)=2.07: ≥58.5 ± 17.8	39.2 ± 8.7 (93.7 ± 3.2)	igneous
4-1 (d-96-E 950 – 1050 m)	738-37	470283	5834950	100s	4	Dpar (μm)=1.34: 55.5 ± 3.2 Dpar (μm)=2.36: 116 ± 10.2	Dpar (μm)=1.34: ≥55.5 ± 3.2 Dpar (μm)=2.36: ≥116 ± 10.2	51.1 ± 2.6	detrital
4-2 (d-96-E 1440 –1525 m)	738-38	470283	5834950	10s	3	Dpar (μm)=1.49: 41.0 ± 3.9	Dpar (μm)=1.49: ≥41.0 ± 3.9	32.4 ± 3.1	detrital
4-3 (d-96-E 2010 – 2150 m)	738-39	470283	5834950	10s	4	Dpar (μm)=1.31: 34.6 ± 5.8 Dpar (μm)=2.00: 38.7 ± 4.9	Dpar (μm)=1.31: ≥34.6 ± 5.8 Dpar (μm)=2.00: ≥38.7 ± 4.9	38.4 ± 4.0	detrital
4-4 (d-96-E 2530 – 2570 m)	738-40	470283	5834950	10s	5	Dpar (μm)=1.25: 45.8 ± 10.4 Dpar (μm)=2.02: 46.4 ± 5.7	Dpar (μm)=1.25: ≥45.8 ± 10.4 Dpar (μm)=2.02: ≥46.4 ± 5.7	48.0 ± 5.3	detrital
4-5 (d-96-E 2810 – 2900 m)	738-41	470283	5834950	100s	5	Dpar (μm)=1.54: 36.9 ± 4.1 Dpar (μm)=2.25: 45.5 ± 9.4	Dpar (μm)=1.54: ≥36.9 ± 4.1 Dpar (μm)=2.25: ≥45.5 ± 9.4	31.4 ± 3.1	detrital
4-6 (d-96-E 525 – 625 m)	738-42	470283	5834950	100s	4	Dpar (μm)=1.48: 60.0 ± 4.8 Dpar (μm)=2.23: 125 ± 19.4	Dpar (μm)=1.48: ≥60.0 ± 4.8 Dpar (μm)=2.23: ≥125 ± 19.4	71.4 ± 4.8	detrital
5-1 (b-22-K 3625 – 3745 m)	738-43	413936	5837969	100s	7	Dpar (μm)=1.68: 6.0 ± 0.8 Dpar (μm)=2.19: 39.8 ± 14.1	Dpar (μm)=1.68: ≥6.0 ± 0.8 Dpar (μm)=2.19: ≥39.8 ± 14.1	12.2 ± 1.5 (50.6 ± 1.6)	mixed (tuffs, argillite)
5-2 (b-22-K 2570 – 2670 m)	738-44	413936	5837969	<10	1	Dpar (μm)=1.83: 40.7 ± 20.4	Dpar (μm)=1.83: ≥40.7 ± 20.4	26.7 ± 13.4 (54.0 ± 2.17)	igneous
5-3 (b-22-K 2020 – 2095 m)	738-45	413936	5837969	<10	1	Dpar (μm)=1.69: 39.3 ± 5.2	Dpar (μm)=1.69: ≥39.3 ± 5.2	33.0 ± 4.4 (52.4 ± 1.6)	igneous
5-4 (b-22-K 1210 – 1280 m)	738-46	480980	5740701	10s	2	Dpar (μm)=1.46: 28.3 ± 3.2	Dpar (μm)=1.56: ≥28.3 ± 3.2	24.1 ± 3.7	igneous
6-1 (b-82-C 1640 – 1700 m)	738-47	480980	5740701	1000s	3	Dpar (μm)=1.85: 102 ± 10.3	Dpar (μm)=1.85: ≥102 ± 10.3	85.5 ± 8.5 (101.4 ± 1.9)	igneous
6-2 (b-82-C 1275 –1320 m)	738-48	480980	5740701	100s	3	Dpar (μm)=1.50: 92.8 ± 8.3 Dpar (μm)=2.16: 93.3 ± 7.0	Dpar (μm)=1.50: ≥92.8 ± 8.3 Dpar (μm)=2.16: ≥93.3 ± 7.0	72.1 ± 4.6	detrital
6-3 (b-82-C 635 –730 m)	738-49	480980	5740701	100s	6	Dpar (μm)=1.55: 46.1 ± 4.3 Dpar (μm)=2.39: 53.6 ± 6.5	Dpar (μm)=1.55: ≥46.1 ± 4.3 Dpar (μm)=2.39: ≥53.6 ± 6.5	37.4 ± 2.9	detrital
6-4 (b-82-C 235 – 300 m)	738-50	480980	5740701	1000s	8	Dpar (μm)=1.70: 38.0 ± 6.9 Dpar (μm)=2.51: 48.5 ± 6.2	Dpar (μm)=1.70: ≥38.0 ± 6.9 Dpar (μm)=2.51: ≥48.5 ± 6.2	41.7 ± 4.5	detrital

TABLE 2 CONTINUED

Field label	A2Z Sample Number	Easting	Northing	Apatite grains observed	Data Quality 1=poor 10=excellent	Age of Oldest Apatite Fission Track (Ma)	Timing of Initiation of Uplift/Cooling (Ma)	Pooled Fission-Track Age (Ma)	Sample type
FF06-10	857-01	357626	5904129	10s	2	Dpar (μm)=1.55: 88.8 ± 19.9	Dpar (μm)=1.55: ≥88.8 ± 19.9	86.6 ± 19.5	detrital
FF06-12	857-02	379434	5932897	100s	4	Dpar (μm)=1.88: 83.7 ± 9.1 Dpar (μm)=2.78: 87.1 ± 36.1	Dpar (μm)=1.88: ≥83.7 ± 9.1 Dpar (μm)=2.78: ≥87.1 ± 36.1	80.4 ± 8.4	detrital
FF06-63	857-03	435864	5912238	100s	5	Dpar (μm)=1.64: 104 ± 6 Dpar (μm)=2.46: 118 ± 7	Dpar (μm)=1.64: ≥104 ± 6 Dpar (μm)=2.46: ≥118 ± 7	107 ± 5.0	detrital
JR06-14	857-06	392951	5918910	100s	1	Dpar (μm)=1.48: 41.2 ± 5.8 Dpar (μm)=2.03: 41.9 ± 4.8	Dpar (μm)=1.48: ≥41.2 ± 5.8 Dpar (μm)=2.03: ≥41.9 ± 4.8	36.2 ± 3.3	detrital
JR06-16	857-07	394086	5918377	100s	1	Dpar (μm)=1.74: 53.2 ± 4.6 Dpar (μm)=2.60: 54.8 ± 1 3.6	Dpar (μm)=1.74: ≥53.2 ± 4.6 Dpar (μm)=2.60: ≥54.8 ± 13.6	53.3 ± 4.4	detrital
JR06-20	857-08	394003	5919332	100s	1	Dpar (μm)=1.61: 49.4 ± 7.2 Dpar (μm)=2.46: 52.2 ± 7.2	Dpar (μm)=1.61: ≥49.4 ± 7.2 Dpar (μm)=2.46: ≥52.2 ± 7.2	49.1 ± 5.0	detrital
JR06-28	857-09	422969	5917545	1000s	9	Dpar (μm)=2.03: 51.2 ± 4.0	Dpar (μm)=2.03: ≥51.2 ± 4.0	52.6 ± 4.1	igneous
JR06-41	857-10	452675	5857782	100s	6	Dpar (μm)=1.75: 30.4 ± 2.5	Dpar (μm)=1.75: ≥30.4 ± 2.5	26.4 ± 2.2	igneous
JR06-77	857-11	476496	5822759	<5	6	Dpar (μm)=1.87: 40.3 ± 8.4	Dpar (μm)=1.87: ≥40.3 ± 8.4	40.4 ± 8.3	detrital
JR07-03	910-01	615061	5955165	1000s	5	Dpar (μm)=2.04: 29.2 ± 4.2	Dpar (μm)=2.04: ≥29.2 ± 4.2	26.6 ± 3.7	detrital
JR07-17	910-02	642922	5956244	1000s	7	Dpar (μm)=1.40: 84.6 ± 7.4	Dpar (μm)=1.40: ≥84.6 ± 7.4	78.1 ± 6.8	igneous
JR07-18	910-03	639801	5955840	10s	6	Dpar (μm)=2.15: 69.1 ± 8.8	Dpar (μm)=2.15: ≥69.1 ± 8.8	64.1 ± 8.2	detrital
JR07-44	910-04	614015	5986720	1000s	6	Dpar (μm)=1.41: 42.2 ± 2.1 Dpar (μm)=2.50: 51.2 ± 5.0	Dpar (μm)=1.41: ≥42.2 ± 2.1 Dpar (μm)=2.50: ≥51.2 ± 5.0	40.7 ± 1.9	detrital
JR07-47	910-05	614667	5990358	1000s	6	Dpar (μm)=1.36: 44.4 ± 2.4 Dpar (μm)=2.08: 47.0 ± 4.1	Dpar (μm)=1.36: ≥44.4 ± 2.4 Dpar (μm)=2.08: ≥47.0 ± 4.1	42.2 ± 2.0	detrital
JR07-62	910-06	619260	5998870	1000s	6	Dpar (μm)=1.62: 46.5 ± 2.5	Dpar (μm)=1.62: ≥46.5 ± 2.5	43.2 ± 2.3	detrital
JR07-64	910-07	621975	5998688	1000s	7	Dpar (μm)=1.25: 109 ± 6 Dpar (μm)=2.20: 120 ± 8	Dpar (μm)=1.25: ≥109 ± 6 Dpar (μm)=2.20: ≥120 ± 8	96.8 ± 4.1	detrital
a-4-L 4800 -– 5305'	965-01	471599	5835406	10s	4	Dpar (μm)=1.490: 49.4 ± 2.8 Dpar (μm)=2.20: 112 ± 6.5	Dpar (μm)=1.490: ≥49.4 ± 2.8 Dpar (μm)=2.20: ≥112 ± 6.5	48.3 ± 2.8	detrital
a-4-L 7180 – 7520'	965-02	471599	5835406	10s	5	Dpar (μm)=1.40: 38.5 ± 3.1 Dpar (μm)=2.42: 57.5 ± 4.8	Dpar (μm)=1.40: ≥38.5 ± 3.1 Dpar (μm)=2.42: ≥57.5 ± 4.8	35.1 ± 2.9	detrital
a-4-L 10625 – 10864'	965-03	471599	5835406	1000s	2	Dpar (μm)=1.80: 26.7 ± 3.0 Dpar (μm)=2.27: 34.7 ± 3.8	Dpar (μm)=1.80: ≥26.7 ± 3.0 Dpar (μm)=2.27: ≥34.7 ±3 .8	16.2 ± 1.8	igneous

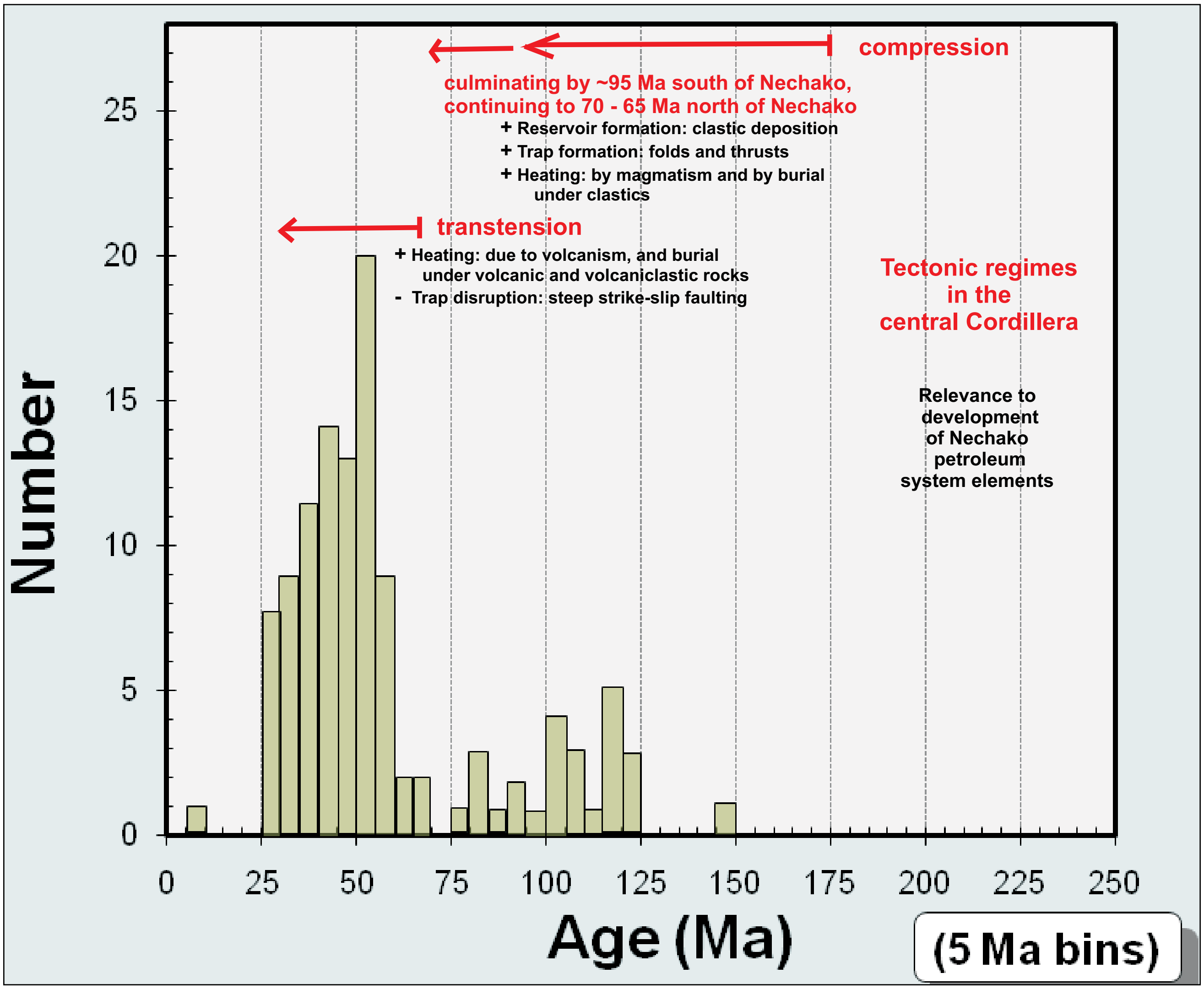

Figure 2. Histogram of ages of oldest apatite fission tracks in Nechako samples. The age of the oldest apatite in a sample is an indication of the last time the sample cooled through the higher end of the apatite annealing temperature range, about 160° C.

ACKNOWLEDGMENTS

All radiometric dates and apatite fission-track analyses were undertaken by Paul O'Sullivan, Raymond Donelick and Margaret Donelick at the Apatite to Zircon Lab of Viola, Idaho. Helpful comments on earlier versions of the manuscript were provided by Fil Ferri, Nathan Hayward, Paul Schiarizza and Paul O'Sullivan.

REFERENCES

Brown, D., Simpson, J., Daniels, H. and Riddell, J. (2008): Petrographic analyses of potential reservoir units of the Nechako region of British Columbia; *BC Ministry of Energy, Mines and Petroleum Resources*, Petroleum Geology Open File 2008-09, 110 pages.

Evenchick, C.A., McMechan, M.E., McNicoll, V.J. and Carr, S.D. (2007): A synthesis of the Jurassic-Cretaceous tectonic evolution of the central and southeastern Canadian Cordillera: exploring links across the orogen; *in* Whence the Mountains? Inquiries into the Evolution of Orogenic Systems; A Volume in Honor of Raymond A. Price, Sears, J.W., Harms, T.A. and Evenchick, C.A., Editors *Geological Society of America*, Special Paper 433, pages 117–145.

Ferri, F. and Riddell, J. (2006): The Nechako Basin project: new insights from the southern Nechako Basin; *in* Summary of Activities 2006, *BC Ministry of Energy, Mines and Petroleum Resources*, pages 89–124.

Friedman, R.M. and Armstrong, R.L. (1988): Tatla Lake metamorphic complex: an Eocene metamorphic complex on the southwestern edge of the Intermontane Belt of British Columbia, *Tectonics*, Volume 7, Number 6, pages 1141–1166.

Grainger, N.C., Villeneuve, M.E., Heaman, L.M. and R.G. Anderson (2001): New U-Pb and Ar-Ar isotopic age constraints on the timing of Eocene magmatism, Fort Fraser and Nechako River map areas, central British Columbia; *Canadian Journal of Earth Sciences*, Volume 38, pages 679–696.

Hayward, N. and Calvert, A. (in prep): Structure of the southeastern Nechako Basin, British Columbia: interpretation of the Canadian Hunter seismic surveys; *Canadian Journal of Earth Sciences*, 2011.

Hickson, C.J. and Higman, S. (1993): Geology of the northwest quadrant, Taseko Lakes map area, west-central British Columbia; *in* Current Research, Part A, *Geological Survey of Canada*, Paper 93-1A, pages 63–67.

Ketcham, R.A., Donelick, R.A., and Carlson, W.D. (1999): Variability of apatite fission-track annealing kinetics: III. Extrapolation to geological time scales, *American Mineralogist*, Volume 84, pages 1235-1255.

Lowe, C., Enkin, R.J. and Struik, L.C. (2001): Tertiary extension in the central British Columbia Intermontane Belt: magnetic and paleomagnetic evidence from the Endako region; *Canadian Journal of Earth Sciences*, Volume 38, pages 657–678.

O'Sullivan, P.B., Evenchick, C.A., Osadetz, K.G., Ferri, F. and Donelick, R.A. (2009): Apatite fission track data for seventeen rocks from the Bowser and Sustut basins, British Columbia; *Geological Survey of Canada*, Open File 6325, 119 pages.

Riesterer, J.W., Mahoney, J.B. and Link, P.K. (2001): The conglomerate of Churn Creek: Late Cretaceous basin evolution along the Insular–Intermontane superterrane boundary, southern British Columbia; *Canadian Journal of Earth Sciences*, Volume 38, Number 1, pages 59–73.

Riddell, J. and Ferri, F. (2008): Nechako Project update; *in* Geoscience Reports 2008, *BC Ministry of Energy, Mines and Petroleum Resources*, pages 67–78.

Riddell, J., Ferri, F., Sweet, A. and O'Sullivan, P. (2007): New geoscience data from the Nechako Basin Project; *in* The Nechako Initiative — Geoscience Update; *BC Ministry of Energy, Mines and Petroleum Resources*, Open File 2007-1, pages 59–98.

Schiarizza, P., Riddell, J., Gaba, R.G, Melville, D.M., Umhoefer, P.J., Robinson M.J., Jennings, B.K. and D. Hick (2002): Geology of the Beece Creek-Nuit Mountain area, B.C. (NTS 92N/8, 9, 10; 92O/5, 6, 12); *BC Ministry of Energy, Mines and Petroleum Resources,* Geoscience Map 2002-3, 1:100 000 scale.

Schiarizza, P., Gaba, R.G., Glover, J.K., Garver, J.I. and Umhoefer, P.J. (1997): Geology and mineral occurrences of the Taseko-Bridge River area; *BC Ministry of Employment and Investment*, Bulletin 100, 292 pages.

Struik, L.C. (1993): Intersecting intracontinental Tertiary transform fault systems in the North American Cordillera; *Canadian Journal of Earth Sciences,* Volume 30, pages 1262–1274.

Tipper, H.W. (1959): Geology, Anahim Lake, British Columbia; *Geological Survey of Canada*, Map 1202, scale 1":4 mi.

Tipper, H.W. (1968): Geology, Mount Waddington, British Columbia; *Geological Survey of Canada*, Map 5-1968, scale 1":2 mi.

Umhoefer, P.J. and Schiarizza, P. (1996): Latest Cretaceous to early Tertiary dextral strike-slip faulting on the southeastern Yalakom fault system, southeastern Coast Belt, British Columbia; *Geological Society of America Bulletin*, Volume 108, Number 7, pages 768–785.